Strojniški vestnik - Journal of Mechanical Engineering 65(2019)7-8, 410-419

DOI:10.5545/sv-jme.2018.5883 Original Scientific Paper
Received for review: 2018-11-23
Received revised form: 2019-04-10
Accepted for publication: 2019-06-17

Images of the Machined Surface in Evaluation of the Efficiency of a Micro-Smoothing Process

Anna Zawada-Tomkiewicz[1,*] – Ryszard Ściegienka[1] – Uros Zuperl[2] – Krzysztof Stępień[3]
[1]Koszalin University of Technology, Poland
[2]University of Maribor, Faculty of Mechanical Engineering, Slovenia
[3]Kielce University of Technology, Poland

The micro-smoothing in this paper concerns belt-grinding operations in two varieties that differ in the use of axial oscillations. The method relies on the continuous slow introduction of the finishing film in the working zone. The film is applied to the rotating workpiece with a defined pressure and axial oscillation. The quality of the machined surface is evaluated as a function of the finishing time.

A model of the belt-grinding efficiency was developed taking into account the machined surface quality. In a monitoring system, an image of the machined surface was applied, decomposed into ten sub-images, which in turn were described by the energy parameter. The decrease of image energy was modelled, and the efficiency of the micro-smoothing process was evaluated, which in turn enabled the estimation of the finishing time. The results confirmed the correctness of the proposed methodology in the analysis of the finishing time of the belt-grinding operations.

Keywords: machining, belt grinding, micro-smoothing, image processing, wavelet analysis

Highlights
- *A model of machined surface formation in micro-machining was developed based on the surface image.*
- *The machining process was evaluated for the purposes of machined surface micro-smoothing.*
- *The discrete wavelet transform DWT components of the machined surface image were applied in process efficiency evaluation.*
- *Optimization of machining time for micro-smoothing and oscillatory micro-smoothing on the basis of the process model was inspected.*

0 INTRODUCTION

Abrasive machining is power-inefficient and time-consuming. It generates a great deal of heat, causing various physical and chemical surface transitions. In **[1]**, the ageing effects on the mechanical and functional properties of resin-bonded grinding wheels were analysed. Grains are held together within a matrix, and their combined shape and density determine the geometry and morphology of the finished workpiece **[2]** and **[3]**.

Abrasion processes are stochastic because the movement and the geometric properties of grains are characterized by sizeable statistical variability. Chen et al. **[4]** developed a method for predicting surface roughness, which takes into account the random distribution of the grain protrusion heights. The material removal in the belt-grinding operations strictly depends on the active cross-sections of the cut layer, which in turn are determined by the interactions between a large number of cutting grains and the workpiece **[5]**. The grains' stochastic geometry, position and even size are the cause of variations in the active cross-sections **[6]** to **[8]**.

The belt-grinding method consists of applying a belt to the face of the rotating workpiece with a defined pressure and axial oscillation. During the finishing film motion, the abrasive grains undergo oscillation at a specific frequency in a direction perpendicular to that of the finishing film motion **[9]** and **[10]**.

The problem concerns the evaluation of the finishing time in which the finishing film is capable of creating the desired micro-topography on the workpiece's surface. The methods embrace the optical evaluation of the tool and workpiece quality in the following categories: whether the tool was correct and used properly with suitable parameters, whether the workpiece topography is achievable with the technology used, and whether the surface image is an appropriate source of information for process evaluation.

In this paper, the two dimensional (2D) discrete wavelet transform was used for the machined surface image to separate the components responsible for roughness and micro-roughness. Analysis of the energy distribution in components enabled the evaluation of the micro-smoothing parameters and the finishing time.

*Corr. Author's Address: Koszalin University of Technology, 15-17 Raclawicka Str, 75-620 Koszalin, Poland, anna.zawada-tomkiewicz@tu.koszalin.pl

1 METHODS

A metallic workpiece made of C45 steel was prepared in the form of a disk. The front face was first ground, and then the finishing process was applied. The finishing process used was belt grinding with IMFF 9 AO 12 mm finishing film (Fig. 1a) [11]. A workpiece was fastened to the self-centring rotary chuck. The face of the workpiece was pressed by the finishing film with 31 N force, which gave a processing zone with a width of 1.8 mm.

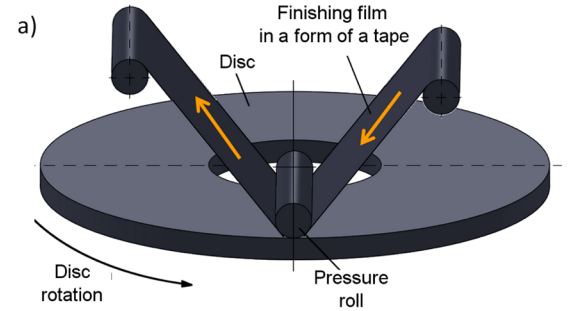

b)

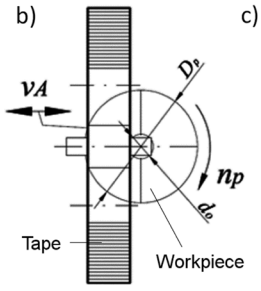

c)

Workpiece diameter	D_p	*mm*	*32*
Speed of workpiece rotation	n_p	rev./min	500
Maximal cutting speed	v_o	mm/min	50.26
Tape feed	v_f	mm/min	80
Cycle machining time	t_1	s	30
Shore's hardness of pressure roll	-	Sh	60
Speed of pressure roll rotation	n_r	rev./min	2.12
Speed of tape oscillations	v_A	mm/min	+/- 1885
Diameter of pressure roll	d_r	mm	12
Speed of worn-out tape rotation	n_{rz}	rev./min	0.8

Fig. 1. *Experimental procedure of the micro-smoothing process; a) schematic view of the operation, b) rectangular projection of the system indicating the direction of the oscillation, c) basic experimental data*

A feature of a belt-grinding method is that the finishing film was used only once in the cutting zone and, after its use, was regarded as worn out. The finishing film is rewound at a low speed from a roll of new finishing film to one with the used film. The finishing film is designed in such a way that the grains moving with the cutting speed are able to cut the material, and the chips are discharged from the cutting zone in the intergranular space. The used finishing film is wrapped on the roll, leaving a clean surface finish. The description above refers to the belt grinding.

In addition to the basic method of belt grinding, a more complex kinematic method was applied, i.e. oscillatory belt grinding (belt grinding with oscillations) (Fig. 1b). The oscillating motion along the surface was applied with the amplitude of 0.5 mm and the frequency of 600 min^{-1} (10 Hz).

The effect of smoothing the machined surface (i.e. obtaining the smallest amplitude parameters of the surface roughness) was emphasized in both processes. Therefore, the article distinguishes micro-smoothing with oscillations and without oscillations. This influenced the methodology of measurements in which the finishing film was exchanged every 30 seconds of the operation, and then the quality of the machined surface was evaluated with the use of a Talysurf CCI 6000 white light interferometer [10] and [12].

1.1 Technology Evaluation

The belt-grinding technology was evaluated with the use of an ECLIPSE MA200 large inverted microscope. The microscope with Nikon CFI 60 optics was used to ensure good image quality of the finishing film and the machined surface.

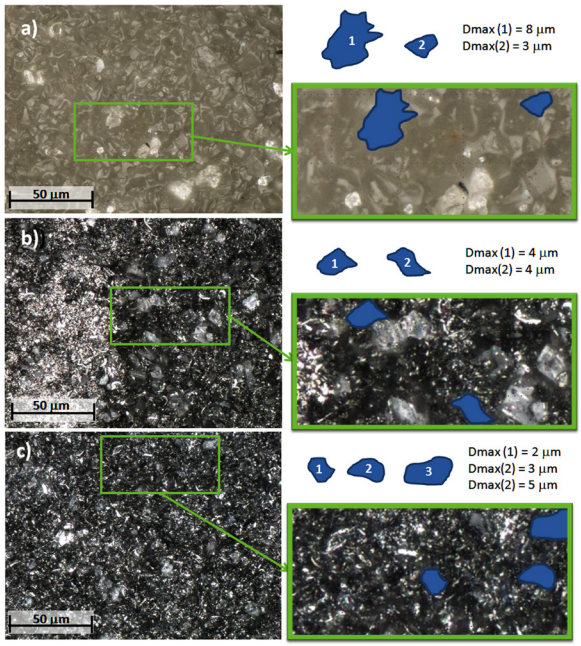

Fig. 2. *Images of finishing film taken with Nikon Eclipse MA 200: a) a new finishing film, b), a finishing film used in a belt-grinding operation (finishing time equal to 2.5 min), c) a finishing film used in a belt-grinding operation with axial oscillations (finishing time equal to 2.5 min)*

Acquisition of the finishing film images and their analysis was difficult due to the properties of the material in which the abrasive grains were embedded. On a new finishing film (Fig. 2a) the abrasive grains

are visible in the form of bright polygons. On the finishing film previously employed in the process (Figs. 2b and c) the single abrasive grains are difficult to distinguish. To facilitate observation, selected abrasive grains were marked.

For the process without oscillations, the abrasive grains work intermittently. They strike the material perpendicularly to the grinding traces, separate or burnish it. Although the grain geometry may vary, the grain tip can still be considered to be characterized by the equivalent radius. This radius typically reflects the sharpness of the grain and how aggressively the cut material can be removed.

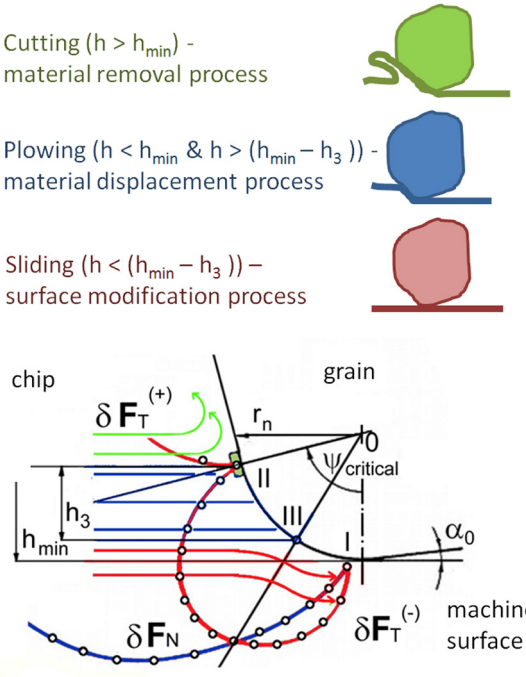

Fig. 3. *Model of the grinding process with force field acting on the rounding of a grain*

In the belt-grinding operations, a natural roundness of grains' edges is a parameter defining the efficiency of the process. It is a result of the mechanism observed during the process, which is, in turn, the consequence of the minimal thickness of the cut layer. When the thickness of cut is smaller than the thickness below which it is unable to form a chip, the grain's active part elastically and plastically deforms the surface. Plowing or rubbing (sliding) is then observed **[13]** and **[14]**. Fig. 3 shows the basics of the process of material removal in the case of small thicknesses of the cut layer.

Oxley **[15]** explained the basics of the process of material removal for a simple case of cutting. At the same time, his research showed that, although in practice, the gains are more geometrically complex, the cutting mechanism for all of them is the same. Cutting, plowing and sliding are the most fundamental interactions in belt-grinding operations, which modify the surface directly and dominate the material removal efficiency.

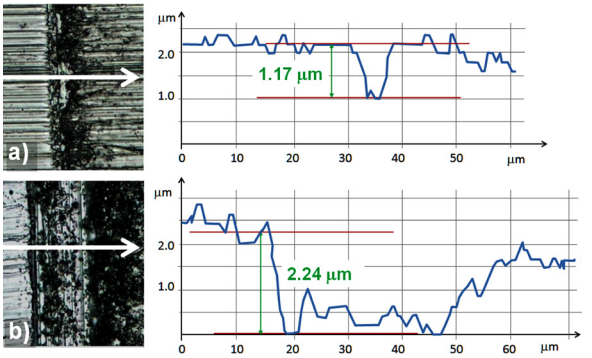

Fig. 4. *Machined surface analysis with the use of Nikon Eclipse MA200 and NIS Elements: a) micro-smoothing process, b) micro-smoothing process with oscillations*

The results of the micro-smoothing process reveal a directionally smooth surface **[2]**, **[3]** and **[10]**. In Fig. 4, the profile along the traces is presented for each micro-smoothing process. The cross-section through the traces of pre-operation demonstrates the process of removing material, where cutting, plowing and sliding are clearly distinguished. When for the belt-grinding process the oscillations are applied, then the abrasive grains are prone to strike the material at different angles, which has a favourable impact on the material removal rate and finally the micro-smoothing effect. This can be seen in Fig. 4b in the form of valley erosion of pre-operation traces.

4.2 Surface Roughness Evaluation

The quality of the machined surface after the belt-grinding process was evaluated with the use of the white light interferometer Talysurf CCI 6000.

Five different regions located along the workpiece radius were measured. In the range of cutting speeds applied, the values for the machined surface along the radius were measured and evaluated. The differences in the values were analysed and found to be statistically insignificant, and thus, they could be treated jointly.

After the belt-grinding operation, the analysis was performed to characterize the influence of the process on the topography of the machined surface. A global analysis of surface topography over the time of belt-grinding operation revealed the micro-smoothing

effect by removing the most protruding peaks of inequalities (Fig. 5).

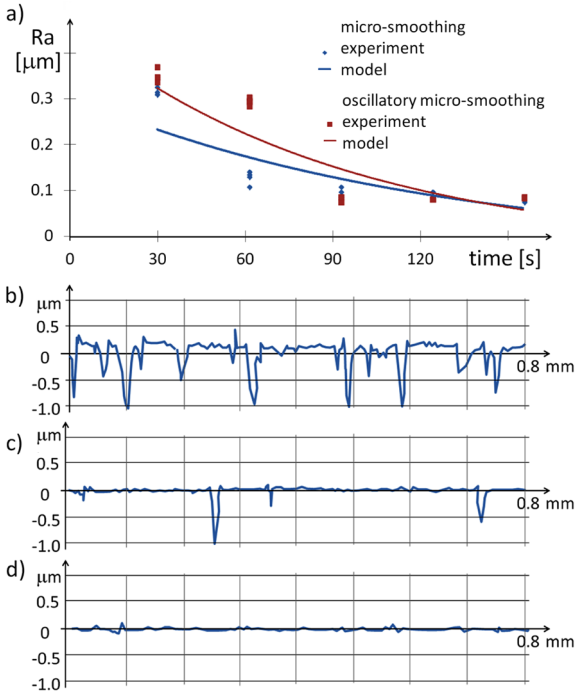

Fig. 5. *Machined surface after the micro-smoothing operation: a) Ra parameter vs machining time, machined surface profile after the micro-smoothing for b) 30 s, c) 90 s, and d) 150 s*

Several different surface roughness parameters were evaluated; two of them are shown in Fig. 6, i.e. *Sa* mean arithmetic surface deviation, *St* total surface height. To determine how different parameters are able to describe the quality of the process, on each of the plots, the values were compared with the surface roughness values obtained for a sufficiently long time of micro-etching.

- When many values were averaged, it turned out that both variations of micro-smoothing lead to the same results in terms of roughness parameters, differing only in the final time after which the parameter value is obtained.
- Despite the fact that in the initial period of micro-cutting, the surface roughness parameter values decrease and the surface becomes smoother (as shown in Fig. 5), this decrease ceases at some point, and under certain conditions no further reduction of the parameter values takes place. The obtained values were presented in the form of a distribution of the actual surface roughness parameters, and the line of 95 % of the average surface roughness values indicates that the surface roughness values should not be expected to be lower than those indicated by the dashed line.

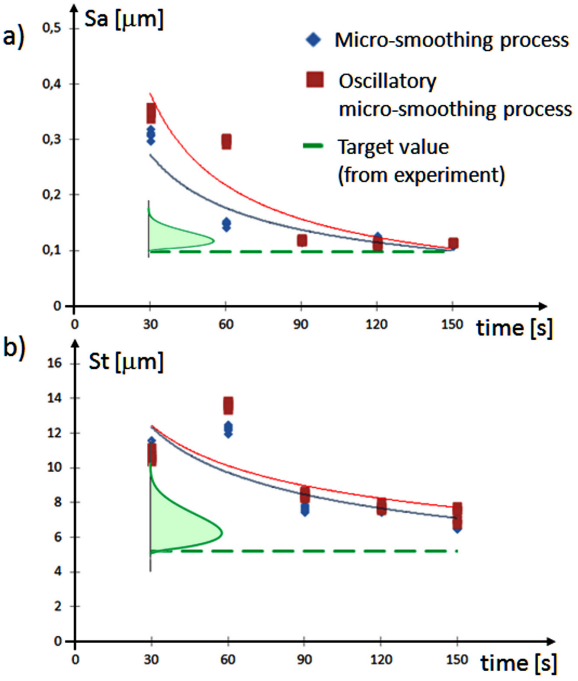

Fig. 6. *Surface roughness area parameters vs finishing time a) Sa parameter, b) St parameter*

2 MODEL OF THE FINISHING PROCESS

Problem definition. The problem defined in this paper is how to carry out the belt-grinding process to efficiently introduce the micro-smoothing of the surface irregularities to obtain the desired quality of the surface finish.

Assumptions. The method of micro-smoothing, shown in Fig. 1, is based on the continuous slow introduction of the finishing film in the working zone. The finishing film is applied to the rotating workpiece with a defined pressure and axial oscillations. The quality of the machined surface is evaluated as a function of the finishing time.

The initial machined surface is in a steady state. The introduction of the belt-grinding process (input signal) changes the output signal (machined surface) from its current value to some other constant value. In a pass of an individual grain, a layer of a thickness not greater than the initial value of the surface roughness will be removed, and the created surface will not be completely new. The created surface will be a modification of the input surface. The minimal value of changes is a function of the minimum thickness of the cut layer depending on the grain and the

workpiece interface. The maximal value of changes is characterized by the cross-section of the cut layer. The belt-grinding process affects the entire surface and changes are observed in surface texture. When changes in the surface texture are small, the process is not efficient, and it should be terminated. The process output signal (machined surface) is observed until a new steady state is reached.

Model. The gain ratio of the model of the micro-smoothing process is determined by the relation of the output signal to the input signal from one steady state to another. An identification of the parameters of the model must describe the character of the process on the basis of the nature of the time response function. Then, on the basis of an approximation of the obtained response of the object, the coefficients of the model are defined [10]. If it is assumed that the process is described by the first-order homogeneous differential equation with the input function in the form of a step function, then a solution is observed in the form of Eq. (1).

$$y(t) = y(t=0)e^{-at} + \frac{b}{a}\left(1-e^{-at}\right) + C_0, \qquad (1)$$

where $y(t)$ is the output value (features of the machined surface). The parameter $1/a$ for $a>0$ can be interpreted as the period T. For $t=T$ we achieve a 63 % steady-state surface (for $t=3T$ we achieve a 95 % steady-state surface). The parameter b/a can be interpreted as gain.

The belt-grinding process is applied for the initial surface with the texture of the pre-operation (the grinding process). Changes in the machined surface gradually lead to the surface finish. Surface parameters change over time, and after a sufficiently long time, they reach the values of C_0.

All analyses of the estimated time of the micro-smoothing process relate to the final effect – the machined surface quality. Belt-grinding process efficiency (throughput) is defined as the output of a process for a unit of time. The efficiency of the smoothing process (Fig. 7a) and the finishing time (Fig. 7b) are presented for a series of successive finishing films. Each of the finishing films can be characterized by the parameter – the equivalent radius of the grain. The removal efficiency of the finishing allowance at each point from the minimum value of the surface parameter to the maximum is different. The finishing time of achieving the machined surface from the range is also different.

The dashed lines in Fig. 7 determine the starting point of the micro-smoothing process and the roughness to be achieved. As can be seen, the range includes micro-smoothing capabilities for the finishing film marked as 1. However, the time to achieve this roughness is long due to the fact that the micro-smoothing efficiency is reduced for the lower roughness. In this case, the final stage of finishing the surface should be carried out using finishing film 2 or 3.

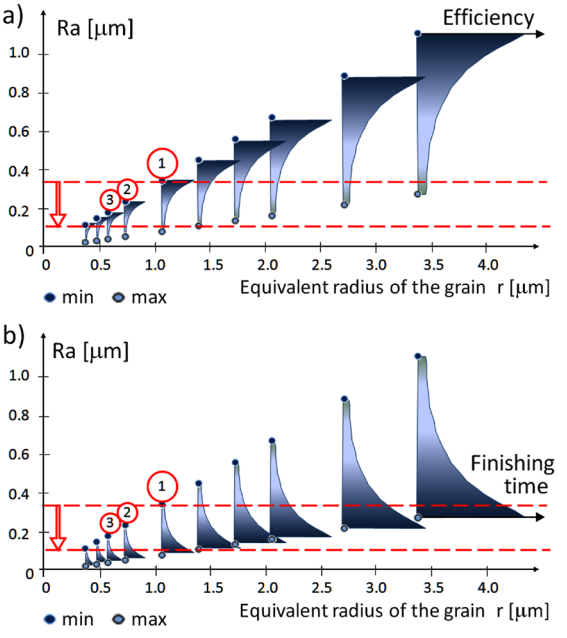

Fig. 7. *Analysis of the efficiency and a) the finishing time, and b) of the micro-smoothing process for a series of successive finishing films*

For an individual finishing film, the micro-smoothing parameters are indicated in relation to the whole decrease in the surface roughness parameters. The use of a finishing film with specific parameters allows the machined surface to be fabricated only in a predetermined range of active cross-sections of the cut layer. The finishing process in which the allowance is smaller is inefficient. An example presented in Fig. 8 shows cross-sections S_1, S_2 and S_3 for which the finishing film should be changed.

The IMFF14 finishing film is used up to the cross-section S_2 and is able to reduce the roughness ΔRa_2. The total reduction of the surface roughness in this example is carried out using three finishing films.

In this article, the analysis of micro-smoothing efficiency is analysed to determine the probability of achieving a given surface roughness with a finishing film. This is done using a digital image of a machined surface, which evaluates the disappearance of the preceding machining traces and the appearance of traces of the finishing operation.

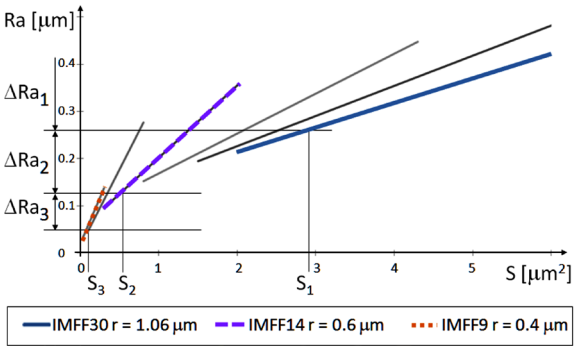

Fig. 8. *Analysis of surface roughness Ra parameter in relation to the active cross-section of the cut layer for a series of successive finishing films*

3 RESULTS AND DISCUSSION

The image of the machined surface was used to evaluate the quality of the machined surface and the finishing time. For successive points in time, digital images of the machined surface were taken, and then, based on the analysis of the identified micro-smoothing traces, the time needed to obtain the assumed final surface was evaluated.

3.1 Surface Image Data Analysis

Surface image data analysis was performed to distinguish the differences in the machined surface image over the time of applying the micro-smoothing process. The algorithm of data processing consisted of three steps. First, the image data were pre-processed [16], then they were decomposed into several significant components, and each of the components was finally evaluated with the energy parameter.

3.1.1 Machined Surface Image

For surface image acquisition, a machine vision system was developed. It consisted of a computer with a frame-grabber card, a digital camera, lenses, a stand for a camera with movable worktable and a surface illumination system. The camera with lenses allows an image of the surface to be obtained with a field of view 1 mm² and depth of view of 100 μm. The surface illumination for the machine vision system was evaluated considering the visibility of both pre-operation and micro-smoothing traces. Four different surface illumination systems were elaborated.

I. Two-sided lighting in the direction perpendicular to the ridges after pre-operation (grinding) and parallel to the ridges after micro-smoothing.
II. Blue and green lighting in the direction perpendicular to the micro-smoothing traces, parallel to the traces of pre-operation.
III. Blue lighting in the direction perpendicular to the micro-smoothing traces, parallel to the traces of pre-operation.
IV. Blue and green lighting in the direction perpendicular to the micro-smoothing traces, parallel to the traces of pre-operation, and double-sided white lighting in the direction perpendicular to the pre-operation and parallel to the traces of micro-smoothing.

Each of the images presented in Table 1 replicates surface texture after the micro-smoothing process. There are two types of intersecting ridges: the traces of grinding and the traces of micro-smoothing, the visibility of which depends on the lighting.

- The first type of surface illumination (I) revealed the traces of the pre-operation. Visible effects of the pre-operation can be seen as ridges, which gradually disappear over the finishing time. First, the traces are shallower, and then their number decreases. Gradually they are replaced by the traces of the belt-grinding process. This type of lighting can be used to analyse the disappearance of traces of pre-operation during the micro-smoothing process.
- The second and third type of surface illumination (II and III) reveal traces of micromachining – different components depending on the colour of light used. The traces of pre-operation are hardly visible in the form of gaps in the traces after micro-smoothing.
- The fourth type of lighting (IV) allows one to observe both traces of the micro-smoothing and traces of the previous operation. Based on the image features of the machined surface obtained over time, it can be concluded that some of the features decrease while others increase. This type of surface illumination was applied for the analyses.

The vision system allowed digital images of surfaces in the process of micro-smoothing to be obtained. These images were analysed using digital image-processing methods. Each of the colour surface images consists of three matrices whose values depend on the adopted colour model. The studies examined the luminance component. A surface image (the luminance component) is a two-dimensional pixel array. The image pixel values themselves refer to grayscales, i.e., the smallest value and the largest value correspond to black and white, respectively. The image data were pre-processed. Three corrections

to the surface image were performed: the noise was removed, the important details were enhanced, and an adjustment for image brightness was made. The procedure for surface image processing was described in [17].

Table 1. *Example images of a machined surface after the micro-smoothing process*

	I	II	III	IV
Micro-smoothing	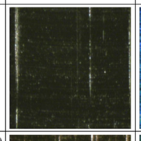	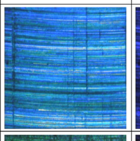	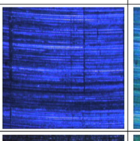	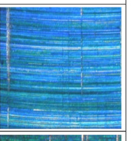
Oscillatory micro-smoothing	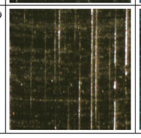	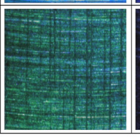	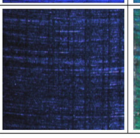	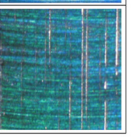

At the output of the image-processing system, a single matrix with dimensions corresponding to the initial image was obtained. Such a data matrix was used in further analyses. The indicator describing the development of the surface in an image is an energy parameter. For a point of a surface image $z=z_{ij}$ depending on spatial variables i and j the energy of the surface image is defined as [14]:

$$Energy = \sum_{i=1}^{N}\sum_{j=1}^{M}\left(z_{ij}\right)^2. \quad (2)$$

The total energy of the machined surface image over the finishing time for micro-smoothing was presented in Fig. 9.

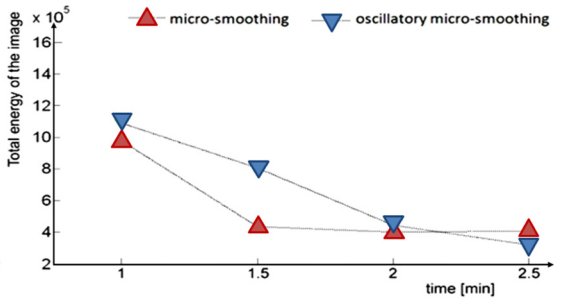

Fig. 9. *Total energy of machined surface image vs micro-smoothing time (the fourth type of surface illumination)*

The initial value of the total energy in both micro-smoothing processes decreases over time. Analysing the energy of a machined surface image as a function of time, one can see how the micro-smoothing process makes the grinding ridges less visible. In each case, the energy is smaller with time. If one tries to analyse the progress of the finishing process basing the judgment on a machined surface image, one can observe two different cases of micro-smoothing parameters.

- The first case concerns micro-smoothing without oscillations. This micro-smoothing process makes the cutting process rapidly remove a large part of the machining allowance when the depth of cut is greater than the minimum (ridges of the pre-operation are deeper). However, when the ridges are shallow, the micro-grinding is difficult because the grains and the free space between grains are sealed up. In this way, the minimal thickness of cut for grains is not achieved, and the material is plastically deformed instead of cut.
- The finishing process supported with oscillations runs in the same way regardless of the pre-operation ridges – each stage of 30 seconds of finishing results in progress of the machined surface image quality (the energy is smaller).

Based on the evolution of the total energy of the machined surface image over time, it is assumed possible to estimate the finishing time. The criterion for achieving the assumed effects is the smoothing of the surface – the disappearance of traces of the pre-operation. However, when choosing the fourth type of surface illumination, the emphasis is placed on a full analysis of traces in different directions. Such analysis requires using appropriate data processing techniques – the 2D discrete wavelet transform (DWT).

3.1.2 Machined Surface Image Decomposition

In the application of image processing, the 2D discrete wavelet transform (DWT) was applied, which provides both frequency and location information on the analysed signal (the resolution and direction in the image) [10], [18] and [19]. The discrete wavelet transform is calculated by applying the one-dimensional transform to rows and columns successively. Firstly the one-dimensional transform is performed on the rows of the image, and then it is applied to the columns of the already horizontally transformed image. The result is decomposed into four matrices having different interpretations.

- The LL matrix consists of all coefficients which were filtered by a low pass filter along the rows and then filtered along the corresponding columns with the low pass filter again. The LL block represents the approximated version of the original image at half the resolution.
- The HL matrix and the LH quadrant consist of the coefficients which were filtered along the rows and columns with the low pass filter and

high pass filter alternately. The LH block contains vertical edges mostly, and the HL block shows horizontal edges.

- The HH matrix was derived with the use of the high pass filter along the rows and then along the columns. The HH block can be interpreted as the area where the edges of the original image in a diagonal direction can be found.

Wavelet decomposition of the machined surface image is presented in Fig. 10. The Meyer wavelet was used as a basic function in the DWT. The components in the transform level n were denoted by $LL(n)$, $LH(n)$, $HL(n)$, and $HH(n)$. Three levels of the DWT were performed, leading to ten independent components. For each surface image component, the energy (Eq. (2)) was calculated.

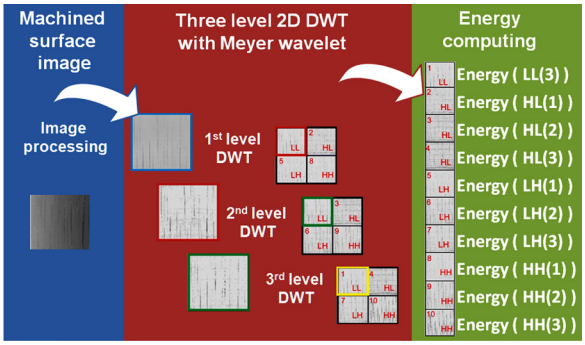

Fig. 10. *Wavelet decomposition of the machined surface image*

Decomposition of the total energy of the image into the energy parameter belonging to individual components allows quantification of the distribution of the data set over the resolutions and directions. The data analysis enables the machined surface image to be divided into a set of DWT components with different energy. Analysis of components with the dominant energy gives an idea of which components create the machined surface image (which resolution and which direction). The energy of the DWT components for a machined surface image enables the comparison of both micro-smoothing processes.

3.2 The Energy of the DWT Components

Images taken during the process of micro-smoothing were analysed with the procedure described in section 2.3 and Fig. 11. The images were decomposed into ten different DWT components. The distribution of the total energy into the DWT components for belt-grinding operation and oscillatory belt-grinding operation is presented in Fig. 11.

The results of the signal energy distribution to individual DWT components show the complexity of the surface texture.

- For the belt-grinding process, large differences in time can be seen for the third level of approximation and vertical components. After the first stage of finishing the decrease in energy is small.
- The decrease in energy for a belt-grinding process with axial oscillation proceeds in a different manner. The decline of the energy parameter over time is more uniform, although greater values are also observed for the third level of approximation and vertical components.

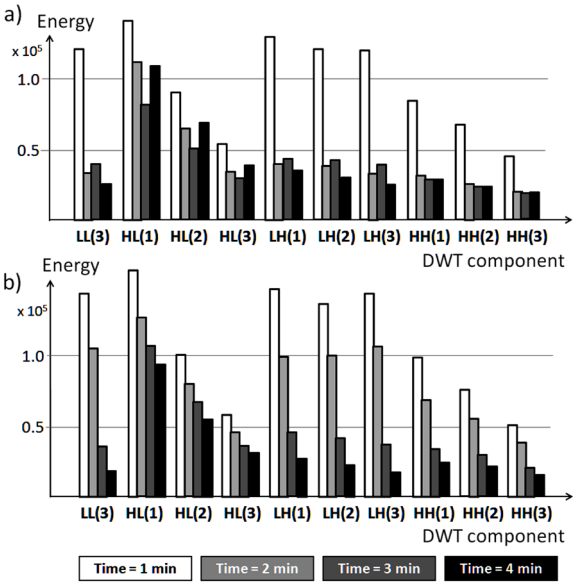

Fig. 11. *The energy of a machined surface image separated into DWT components a) for micro-smoothing, b) for micro-smoothing with oscillations*

Analysis of the finishing time was performed to minimize the energy contained in each component of the machined surface image. Changes in the energy of individual DWT components of the surface image were modelled in accordance with the procedure presented in Chapter 2 using Eq. (1). On this basis, the time of obtaining the assumed surface quality was calculated. The values of the estimated finishing time are shown in Fig. 12. If only the approximated signal, referring to the low-resolution components, is analysed, then the estimated time would be as short as 4 to 5 minutes. Analysis of surface image details in different resolutions and in different directions indicates that the finishing time should be much longer.

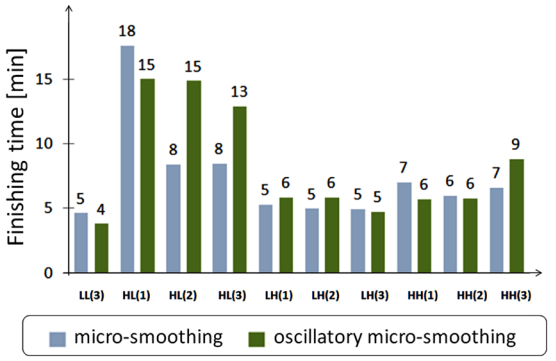

Fig. 12. *Estimated time of micro-smoothing process calculated on the basis of a model of energy distribution for the DWT components of the surface image*

The three cases can be considered in relation to the finishing time: the times when 50 %, 68 % and 95 % of the surface quality was achieved.

- The average time to obtain 50 % of the assumed surface accuracy is 7 minutes in the case of micro-smoothing and 8.7 minutes in the case of oscillatory micro-smoothing.
- Assuming that the finishing film should be changed when the desired effect has been obtained with a probability of 68 %, the time is similar for both micro-smoothing processes and amounts to approximately 12 minutes.
- When the micro-smoothing is a finishing process, the final roughness should correspond to 95 % of the assumed surface accuracy that is possible under the given conditions. The machining time was estimated to be not less than 17 minutes for the micro-smoothing and 14 minutes for the oscillatory micro-smoothing.

4 CONCLUSIONS

The efficiency of the belt-grinding operation depends on the parameters of the finishing process in relation to the initial surface and the machined surface after the process of micro-smoothing. In this paper, micro-smoothing and the oscillatory micro-smoothing were applied for relatively soft C45 steel after the process of grinding.

The machined surface after the micro-smoothing process was expected to be very smooth. The quality of the machined surface was evaluated with the use of a Talysurf CCI 6000 and a machine vision system. The machined surface roughness parameters were used for system evaluation, and the machined surface images were applied for the estimation of finishing time.

Machined surface images were pre-processed and then decomposed with the use of the 2D DWT. The components of the wavelet decomposition were analysed in relation to the possibility of evaluating the time of micro-smoothing processes.

Individual components of the DWT were evaluated, taking into account the process efficiency and the finishing time. A significant decrease in image energy was observed for the approximation component LL(3) and the vertical components LH(1), LH(2) and LH(3). Nevertheless, the micro-smoothing for all the examined cases proved to have a favourable influence on the machined surface parameters. The best results (considering Fig. 12) were achieved for the micro-smoothing with axial oscillation, because the uniform reduction of the components caused not only significant energy reduction in the vertical, detail and approximation components (as was expected) but also a reduction of energy in the horizontal components.

6 ACKNOWLEDGEMENTS

The paper has been prepared under the research project entitled "Theoretical and experimental problems of integrated 3D measurements of elements' surfaces", reg. no.: 2015/19/B/ST8/02643, ID: 317012, financed by the National Science Centre, Poland.

5 REFERENCES

[1] Matavž, A., Mursics, J., Anzel, I., Zagar, T. (2018). The influence of external conditions on the mechanical properties of resin-bonded grinding wheels. *Strojniški vestnik - Journal of Mechanical Engineering*, vol. 64, no. 7-8, p. 453-464, **DOI:10.5545/sv-jme.2017.5083**.

[2] Grzesik, W., Rech, J., Wanat, T. (2007). Surface finish on hardened bearing steel parts produced by superhard and abrasive tools. *International Journal of Machine Tool & Manufacture*, vol. 47, no 2, p. 255-262, **DOI:10.1016/j.ijmachtools.2006.01.009**.

[3] Jourani, A., Dursapt, M., Hamdi, H., Rech, J., Zahouani, H. (2005). Effect of the belt grinding on the surface texture: Modeling of the contact and abrasive wear. *Wear*, vol. 259, no. 7-12, p. 1137-1143, **DOI:10.1016/j.wear.2005.02.113**.

[4] Chen, H., Tang, J., Zhou, W. (2013). Modeling and prediction of surface roughness for generating grinding gear. *Journal of Materials Processing Technology*, vol. 213, no. 5, p, 717-721, **DOI:10.1016/j.jmatprotec.2012.11.017**.

[5] Zhang, Y. Fang, C., Huang, G., Xu, X. (2018). Modeling and simulation of the distribution of undeformed chip thicknesses in surface grinding. *International Journal of Machine Tools and Manufacture*, vol. 127, p. 14-27, **DOI:10.1016/j.ijmachtools.2018.01.002**.

[6] Deiva Nathan, R., Vijayaraghavan, L., Krishnamurthy, R. (1999). In-process monitoring of grinding burn in

cylindrical grinding of steel. *Journal of Materials Processing Technology*, vol. 91, no. 1-3, p. 37-42, **DOI:10.1016/S0924-0136(98)00408-7**.

[7] Lipiński, D., Kacalak, W.(2016). Metrological Aspects of Abrasive Tool Active Surface Topography Evaluation. *Metrology & Measurement Systems*, vol. 23, no (4) p. 567-577, **DOI:10.1515/mms-2016-0043**.

[8] Mezghani S., El Mansori, M. (2008). Abrasiveness properties assessment of coated abrasives for precision belt grinding. *Surface & Coatings Technology*, vol. 203, no. 5-7, p. 786-789, **DOI:10.1016/j.surfcoat.2008.08.058**.

[9] Lewkowicz, R., Kacalak, W., Ściegienka, R., Bałasz, B. (2009). The new methods and heads for precision microfinishing with application of microfinishing films. *Proceedings of the 5th International Congress on Precision Machining*.

[10] Zawada-Tomkiewicz, A., Ściegienka, R. (2011). Monitoring of the micro-smoothing process with the use of machined surface image. *Metrology and Measurement Systems*, vol. 18, no. 3, p. 419-428, **DOI:10.2478/v10178-011-0008-8**.

[11] Reference materials of microfinishing film, from: *http://www.ussupplyinc.com/products/3m.html.*

[12] Kacalak, W., Różański, R., Lipiński, D. (2016). Evaluation of classification ability of the parameters characterizing stereometric properties of technical surfaces. *Journal of Machine Engineering*, vol. 16, no. 2, p. 86-94.

[13] Mezghani, S., El Mansori, M., Zahouani, H. (2009). New criterion of grain size choice for optimal surface texture and tolerance in belt finishing production. *Wear*, vol. 266, no. 5-6, p. 578-580, **DOI:10.1016/j.wear.2008.04.074**.

[14] Storch, B., Zawada-Tomkiewicz, A. (2012) Distribution of unit forces on the tool edge rounding in the case of finishing turning. *The International Journal of Advanced Manufacturing Technology*, vol. 60, no. 5-8, p. 453-461, **DOI:10.1007/s00170-011-3617-7**.

[15] Oxley, P.L.B. (1989). *The Mechanics of Machining: An Analytical Approach to Assessing Machinability*, Ellis Horwood, Chichester.

[16] Zuperl, U., Cus, F. (2015). Simulation and visual control of chip size for constant surface roughness. *International Journal of Simulation Modelling*, vol. 14, no. 3, p. 392-403, **DOI:10.2507/IJSIMM14(3)2.282**.

[17] Simunovic, G., Svalina, I., Simunovic, K., Saric, T., Havrlisan, S., Vukelic, D. (2016). Surface roughness assessing based on digital image features. *Advances in Production Engineering & Management*, vol. 11, no. 2, p. 93-104, **DOI:10.14743/apem2016.2.212**.

[18] Adamczak, S., Makieła, W. (2011). Analyzing the variations in roundness profile parameters during the wavelet decomposition process using the MATLAB environment. *Metrology & Measurement Systems*, vol. 18, no. 1, p. 25-34, **DOI:10.2478/v10178-011-0003-6**.

[19] Zawada-Tomkiewicz, A. (2010). Estimation of surface roughness parameter based on machined surface image. *Metrology and Measurement Systems*, vol. 17, no. 3 p. 493-504, **DOI:10.2478/v10178-010-0041-5**.